A New Mixed Iterative Algorithm to Solve the Fuel-Optimal Linear Impulsive Rendezvous Problem

D. Arzelier, C. Louembet, A. Rondepierre & M. Kara-Zaitri

Journal of Optimization Theory and Applications

ISSN 0022-3239

J Optim Theory Appl
DOI 10.1007/s10957-013-0282-z

Springer

J Optim Theory Appl
DOI 10.1007/s10957-013-0282-z

A New Mixed Iterative Algorithm to Solve the Fuel-Optimal Linear Impulsive Rendezvous Problem

D. Arzelier · C. Louembet · A. Rondepierre · M. Kara-Zaitri

Received: 13 April 2012 / Accepted: 12 February 2013

Abstract The optimal fuel impulsive time-fixed rendezvous problem is reviewed. In a linear setting, it may be reformulated as a non-convex polynomial optimization problem for a pre-specified fixed number of velocity increments. Relying on variational results previously published in the literature, an improved mixed iterative algorithm is defined to address the issue of optimization over the number of impulses. Revisiting the primer vector theory, it combines variational tests with sophisticated numerical tools from algebraic geometry to solve polynomial necessary and sufficient conditions of optimality. Numerical examples under circular and elliptic assumptions show that this algorithm is efficient and can be integrated into a rendezvous planning tool.

Keywords Orbital rendezvous · Fuel optimal space trajectories · Primer vector theory · Impulsive maneuvers · Linear equations of motion

1 Introduction

Given the increasing need for satellite servicing in current and future space programs developed in conjunction with rendezvous missions for the International Space Sta-

Communicated by Bruce A. Conway.

D. Arzelier (✉) · C. Louembet · M. Kara-Zaitri
CNRS, LAAS, 7 avenue du colonel Roche, 31400 Toulouse, France
e-mail: arzelier@laas.fr

D. Arzelier · C. Louembet · M. Kara-Zaitri
Université de Toulouse, LAAS, 31400 Toulouse, France

A. Rondepierre
IMT, 118 route de Narbonne, 31400 Toulouse, France

Published online: 27 February 2013

tion (ISS), the interest of most space agencies in developing adequate rendezvous mission planning tools has been rising rapidly. In particular, new challenges related to the synthesis of guidance schemes have appeared. Among those challenges, the capacity of achieving autonomous far range rendezvous on highly elliptical orbits, while preserving optimality in terms of fuel consumption, is fundamental. Strictly speaking, the space far range rendezvous maneuver is an orbital transfer between a passive target and an actuated spacecraft called "the chaser", within a fixed or floating time period. In this paper, we mainly focus on the so-called time-fixed fuel optimal rendezvous problem in a linearized gravitational field, for which a renewed interest has been witnessed in the literature [1–4]. Numerical solutions based on linear relative motion are particularly appealing when dealing with on-board guidance algorithms. Indirect approaches based on the solution of optimality conditions derived from Pontryagin's Maximum Principle, leading to the development of the so-called primer vector theory presented in [5], have been an avenue of research in numerous studies [6–9]. As they only focus on fixed number of impulses, these approaches fail to optimize trajectory planning in terms of number of impulsive maneuvers. In [8], an iterative heuristic procedure is shortly described to consider optimization over thrust positions in the circular case, while [10] extends it to the elliptic case. To optimize the number of impulses as well as their specific application times, an iterative algorithm based on the calculus of variations, originally developed by Lion and Handelsman [11], has been designed in [12–14]. The main drawback, however, is due to the possible non-smoothness and sub-optimality of the resultant trajectory of the primer vector norm. To overcome this difficulty, a Davidon–Fletcher–Powell penalty minimization step is proposed in order to move the impulses and achieve a smooth optimal trajectory, as detailed in [13–15].

The paper's contribution is to revisit the iterative algorithm of Lion–Handelsman, by taking advantage of the polynomial nature of the underlying necessary conditions, to circumvent the necessity to resort to local optimization schemes. In [16], a new algorithm, based on polynomial optimization, is proposed to tackle the problem of fixed-time impulsive linear rendezvous for a fixed number of impulses. A certificate of global optimality is built with the optimal solution. A heavy time-consuming dynamic gridding of thrust locations is performed in order to determine the optimal impulses for a fixed number of maneuvers. While [16] gives optimal solution for a fixed number of impulses, this new algorithm converges to the minimum-fuel solution over the number of impulses via an iterative process. The heavy gridding process is avoided by obtaining the optimal locations at the end of the convergence process. At each step, this iterative process solves some of the necessary conditions (polynomial system of equations) without solving the complete nonlinear non-convex polynomial optimization problem via a hierarchy of relaxations. For complex instances, the order of relaxation necessary to build the optimal solution may be high and numerically out of reach. The new proposed iterative algorithm combines powerful numerical tools from the algebraic geometry field and very simple rules derived from the variational tests defined in [11] to iteratively improve a non optimal preliminary solution. In contrast with the original iterative algorithm developed in [13, 15] or [14], this procedure builds a successive, always-improving, suboptimal solutions, verifying necessary conditions of smoothness of the derivative of the norm of the primer vector, at each step. Therefore, a cusp occurrence is impossible, and there is no need for the usual local optimal search step bypassing the usual problems of initialization, convergence to local minima different from zero or the plateauing phenomenon. In addition, the cases for which an initial two-impulse solution does not exist may be tackled in a similar way. Finally, Hill–Clohessy–Wiltshire [17] or Tschauner–Hempel [18] relative models for the primer vector dynamics may be considered indifferently, while the algorithms in [13, 15] or [14] are restricted to the first one.

In the first section of this paper, the framework of the minimum-fuel fixed-time rendezvous problem is presented, and necessary and sufficient conditions of optimality are recalled. Relative dynamics motion for rendezvous are the well-known Tschauner–Hempel equations [18] and the transition matrix of Yamanaka–Ankersen [19]. The results of [11] are recalled, and the mixed iterative algorithm is presented. For the sake of comparison, the efficiency of the proposed algorithms is illustrated with three different numerical examples. First, an academic example taken from Carter's reference [8] is studied in detail. Furthermore, two realistic scenarios based on the ATV program [20] and on the PRISMA "technology in-orbit testbed mission", demonstrating formation flight [3], are also reviewed.

2 The Time-fixed Optimal Rendezvous Problem

2.1 Linear Impulsive Time-fixed Optimal Rendezvous Problem

This paper focuses on the fixed-time minimum-fuel rendezvous between close orbits of an active (actuated) spacecraft, called the chaser, with a passive target spacecraft, assuming a linear impulsive setting, and a Keplerian relative motion, as it is defined in [8, 9]. The impulsive approximation for the thrust means that instantaneous velocity increments are applied to the chaser whereas its position is continuous. If the relative equations of motion of the chaser are supposed to be linear and under the previous Keplerian assumptions, it is shown in [8–10] that the considered minimum-fuel rendezvous problem may be reformulated as the following optimization problem:

$$\begin{aligned} &\min_{N,\theta_i,\Delta v_i,\beta(\theta_i)} \quad J = \sum_{i=1}^{N} \Delta v_i \\ &\text{s.t.} \quad u_f = \sum_{i=1}^{N} \phi^{-1}(\theta_i) B(\theta_i) \Delta v_i \beta(\theta_i) = \sum_{i=1}^{N} R(\theta_i) \Delta v_i \beta(\theta_i), \\ &\qquad \|\beta(\theta_i)\| = 1, \\ &\qquad \Delta v_i \geq 0, \end{aligned} \tag{1}$$

where $\phi(\theta)$ is the fundamental matrix associated to the linearized relative free motion and $\Phi(\theta, \theta_1) = \phi(\theta)\phi^{-1}(\theta_1)$ denotes, therefore, the transition matrix of the linearized relative free motion. Note that the true anomaly θ has been chosen as the independent variable throughout in the paper. θ_0 and θ_f respectively denote the initial and final values of the true anomaly during the rendezvous. $u_f = \phi^{-1}(\theta_f)X_f - \phi^{-1}(\theta_1)X_0 \neq 0$, where the state vector $X_f = [r_f^T \quad v_f^T]^T$ at θ_f and the state vector $X_0 = [r_0^T \quad v_0^T]^T$ at θ_0 are composed of the relative positions and relative velocities vectors. The optimization decision variables are the number of impulses N, the sequence of thrust locations $\{\theta_i\}_{i=1,\dots,N}$, the sequence of thrust magnitudes $\{\Delta v_i\}_{i=1,\dots,N}$ and of thrust directions $\{\beta(\theta_i)\}_{i=1,\dots,N}$. Due to the lack of a priori information about the optimal number of impulses to be considered, problem (1) is very hard to solve from both theoretical and numerical points of view. Therefore, the associated fixed-time minimum-fuel rendezvous problem for a fixed number N of impulses has been considered in the literature mainly via geometric methods near circular [6, 15, 21] or elliptic [10] orbits. These results are mainly based on the derivation of optimality conditions for the problem (1) when N is fixed a priori.

2.2 Carter's Necessary and Sufficient Conditions for a Fixed Number of Impulses

When the number of impulses is not a part of the optimization process and is fixed a priori to N, problem (1) may be considered as the joint optimal selection of N velocity increments $\Delta V(\theta_i) = \Delta v_i \beta(\theta_i)$ and N times θ_i of maneuvers. By applying a Lagrange multiplier rule for the problem (1) as in [10], one can derive necessary conditions of optimality (2) to (6) in terms of the Lagrange multiplier vector $\lambda \in \mathbb{R}^n$, as is recalled in Theorem 2.1 below. Prussing has first shown in [22] that these conditions are also sufficient in the case of linear relative motion with the strengthening semi-infinite constraint (9) that should be fulfilled on the continuum $[\theta_0, \theta_f]$ and is expressed in terms of the matrix $R(\theta)$.

Theorem 2.1 (Carter [9]) $(\theta_1, \dots, \theta_N, \Delta v_1, \dots, \Delta v_N, \beta(\theta_1), \dots, \beta(\theta_N))$ *is the optimal solution of problem* (1) *if and only if there exists a non-zero vector* $\lambda \in \mathbb{R}^m$, $m = \dim(\phi)$ *that verifies the necessary and sufficient conditions*:

$$\Delta v_i = 0 \quad \text{or} \quad \beta(\theta_i) = R^T(\theta_i)\lambda, \quad \forall i = 1, \dots, N, \tag{2}$$

$$\Delta v_i = 0 \quad \text{or} \quad \lambda^T R(\theta_i) R(\theta_i)^T \lambda = 1, \quad \forall i = 1, \dots, N, \tag{3}$$

$$\Delta v_i = 0 \quad \text{or} \quad \theta_1 = \theta_0 \quad \text{or} \quad \theta_N = \theta_f \quad \text{or} \quad \lambda^T \frac{dR(\theta_i)}{d\theta} R(\theta_i)^T \lambda = 0,$$

$$\forall i = 1, \dots, N, \tag{4}$$

$$\sum_{i=1}^{N} \big[R(\theta_i) R^T(\theta_i)\big] \lambda \Delta v_i = u_f, \tag{5}$$

$$\Delta v_i \geq 0, \quad \forall i = 1, \dots, N, \tag{6}$$

$$\sum_{i=1}^{N} \Delta v_i = u_f^T \lambda > 0, \tag{7}$$

$$u_f^T \lambda \text{ is the minimum of the set defined as } \left\{\lambda \in \mathbb{R}^m : (2)\text{–}(7) \text{ are verified}\right\}, \tag{8}$$

$$\left\|\lambda_v(\theta)\right\| \leq 1, \quad \forall \theta \in [\theta_1, \theta_N], \tag{9}$$

where $\lambda_v(\theta) = R(\theta)^T \lambda$ *denotes the so-called primer vector.*

Note that conditions (7) and (8) may be easily derived from the previous ones. These results derive directly from the seminal work of [5] in the early 1960s, and form an alternative formulation to the primer vector theory.

A numerical solution of optimality conditions (2)–(9) in the unknowns $\lambda \in \mathbb{R}^m$, $\{\theta_i\}_{i=1,\dots,N}$, $\{\beta(\theta_i)\}_{i=1,\dots,N}$, $\{\Delta v_i\}_{i=1,\dots,N}$ is still hard to find for a fixed number of impulses N, due to the non-convex and transcendental nature of these polynomial equalities and inequalities. However, it is shown in [16] that the problem may be tackled by using an adequate dynamic gridding strategy and polynomial optimization. Still, the optimal number of impulses N^* for a particular rendezvous problem is generally unknown, and only a bound $N^* \leq N_{\max}$ is available [23]. $N_{\max} = 2$ for out-of-plane rendezvous [7], $N_{\max} = 4$ for in-plane rendezvous while $N_{\max} = 6$ for a general three-dimensional rendezvous problem. Apart from the gridding step, the necessity to try every case for $2 \leq N \leq N_{\max}$ in [16] appears be very time-consuming, and a more direct approach to solve problem (1) is now proposed.

3 Optimizing over the Number of Impulses

3.1 Using Lion & Handelsman Results on Multi-impulse Trajectories

In [11], a method is proposed to take advantage of the primer vector theory, developed by Lawden, in order to improve non-optimal trajectories by adding or shifting impulses. The calculus of variations is used to find conditions on the norm of the primer vector for an additional impulse and on the derivative of this norm for initial and/or final coastings. The method is mainly based on derivation of the so-called *variational adjoint equation* resulting from the variation of the cost function. Later, Jezewski [12, 13] and Prussing in [14] developed a numerical algorithm, combining Lion–Handelsman's conditions with a modified gradient search approach to the problem in an inverse square gravitational field. The additional local optimization procedure is used to find the optimal position and modulus of the additional impulse and prevent a resulting cusp for the norm of the primer vector, as reported in [12, 13]. In this section, the conditions of Lion and Handelsman are recalled, and a different heuristic iterative procedure avoiding local optimal search step and cusp occurrence is proposed. It is worth noticing that the extension of these conditions for elliptical reference orbit (Tschauner–Hempel [18] dynamical relative model and Yamanaka–Ankersen transition matrix [19]) from [24] is used here.

3.1.1 Additional Interior Impulse Condition

Perturbing a reference initial two-impulse trajectory and adding an interior impulse at θ_m, the differential cost can be expressed as:

$$\delta J = \Delta v_m \big(1 - \lambda_v(\theta_m)^T \beta(\theta_m)\big) = \Delta v_m \big(1 - \lambda^T R(\theta_m)\beta(\theta_m)\big). \tag{10}$$

From (10), it is easy to conclude that $\delta J < 0$ when $\|\lambda_v(\theta_m)\| > 1$ and that a maximum decrease in cost is obtained when:

$$\theta_m = \arg \max_{\theta \in [\theta_0, \theta_f]} \big\|\lambda_v(\theta)\big\| = \arg \max_{\theta \in [\theta_0, \theta_f]} \big\|R^T(\theta)\lambda\big\|. \tag{11}$$

3.1.2 Additional Coasting Period Conditions

For an additional initial coasting period of duration $d\theta_1$, the cost variation is given by:

$$\begin{aligned}\delta J = -\Delta v_1 \frac{d\lambda_v}{d\theta}^T(\theta_1)\lambda_v(\theta_1)d\theta_1 &= -\Delta v_1 \lambda^T \frac{dR}{d\theta}(\theta_1)R^T(\theta_1)\lambda d\theta_1 \\ &= \Delta v_1^2 \frac{d\|\lambda_v(\theta)\|}{d\theta}_{|\theta=\theta_1} d\theta_1.\end{aligned} \tag{12}$$

This condition means that adding an initial coasting arc of $d\theta_1 > 0$ duration may improve the cost if $\dot{\lambda}_v(\theta_1)^T \lambda_v(\theta_1) > 0$, i.e., the right derivative of the primer vector norm at θ_1 is positive. Similarly, for a final coasting arc of duration $d\theta_f$, we get:

$$\begin{aligned}\delta J = -\Delta v_f \frac{d\lambda_v}{d\theta}(\theta_f)^T \lambda_v(\theta_f)d\theta_f &= -\Delta v_f \lambda^T \frac{dR}{d\theta}(\theta_f)R^T(\theta_f)\lambda d\theta_f \\ &= -\Delta v_f^2 \frac{d\|\lambda_v(\theta)\|}{d\theta}_{|\theta=\theta_f} d\theta_f.\end{aligned} \tag{13}$$

A final coast of $d\theta_f < 0$ duration will improve the cost when the left derivative of the primer vector norm at θ_f is negative, i.e., when $\frac{d\lambda_v}{d\theta}(\theta_f)^T \lambda_v(\theta_f)$.

3.2 A Mixed Iterative Algorithm

These conditions may be used jointly to reduce the cost of a reference non-optimal two-impulse trajectory, but can also be generalized to multi-impulse trajectories.

As noted in [12] and in [25], computation of the mid-impulse might nevertheless results in a non-optimal trajectory not verifying the optimality conditions of Lawden and condition (9), particularly in the case of occurrence of a cusp at θ_m, as illustrated in Fig. 1. A particular strategy combining Lion–Handelsman's conditions and local direct optimization based on the Davidon–Fletcher–Powell penalty method in [13] or based on BFGS method in [25] has been proposed to optimize the resulting three-impulse trajectory. The objective of this section is to propose an alternative to this complicated procedure by developing a mixed iterative algorithm, taking

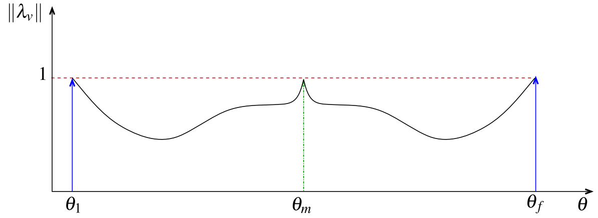

Fig. 1 Non-optimal primer vector norm with a cusp at the interior impulse

advantage of the algebraic formulation of Carter's optimality conditions and of the Lion–Handelsman's conditions. Starting from a non-optimal two-impulse trajectory, successive admissible improved trajectories will be iteratively built by:

- Adding impulse at θ_m if the impulse number does not exceed the upper bound $N_{\max}$;
- Moving the proximal impulse to θ_m if an impulse cannot be added due to $N = N_{\max}$;
- Merging two impulses at θ_m if there is no proximal impulse and if an impulse cannot be added due to $N = N_{\max}$,

where θ_m is defined by (11). The logic of the proposed heuristic algorithm is depicted at Fig. 2, where $dp_i = \frac{d\|\lambda\|}{d\theta}(\theta_i)$ and $dp_{i+1} = \frac{d\|\lambda\|}{d\theta}(\theta_{i+1})$. The set T_{imp} denotes the current set impulses and the new impulse θ_m is always added to it.

This heuristic procedure relies on basic principles that are used to make the successive sequences of maneuvers monotonically converging to an optimal solution.

- The first and final maneuvers locations, defined respectively at θ_0 and θ_f, cannot be moved in the process. Therefore, optimal solutions consisting of an initial and/or final coasting period cannot be found by this algorithm.
- A new impulse is always added at θ_m. In case 8 for an actual number of impulses $N < N_{\max}$, it increases the number of impulses, while when $N = N_{\max}$, it reduces the number of impulses in cases 3 and 7, and it does not change this number for cases 1, 2, 4, 5, and 6.
- Every move of an actual maneuver time to θ_m is chosen to be the proximal of θ_m (in particular for case 4), except in case 7, which is specific since moves of impulses θ_i and θ_{i+1} are not required to improve the trajectory. In this case, the idea is rather to re-initialize the iterative process with a new three-impulse trajectory. In practice, this case has never occurred on all the tested numerical examples.

The systematic convergence of the algorithm for any rendezvous is not analytically proven, but no different case has been reported in the different numerical tests performed so far.

The algorithm may now be described in details. It is mainly composed of two stages: One initialization step solving a two-impulse rendezvous problem, and the iterative procedure building the final plan of maneuvers. ϵ_{cond} and ϵ_λ are respectively the precision values on the conditioning number of the transition sub-matrix Φ_{12}, and on the maximum of the norm of the primer vector. Typically, $\epsilon_{\text{cond}} = 10^6$ while $\epsilon_\lambda = 10^{-6}$.

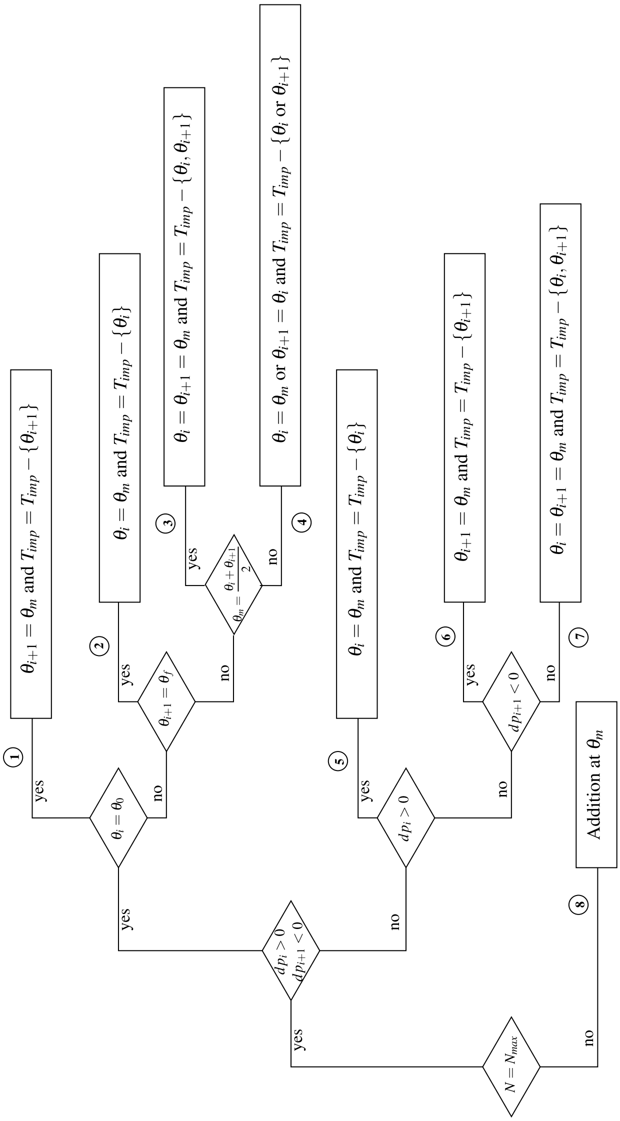

Fig. 2 Heuristic for the mixed iterative algorithm

Initialization step:

(a) **Solve** the two-impulse problem:
1. **Initialize**

$$T_{\text{imp}} = \{\theta_1, \theta_2\} = \{\theta_0, \theta_f\}. \tag{14}$$

2. **Compute** the transition matrices

$$\Phi(\theta_f, \theta_1) = \begin{bmatrix} \Phi_{11}(\theta_f, \theta_1) & \Phi_{12}(\theta_f, \theta_1) \\ \Phi_{21}(\theta_f, \theta_1) & \Phi_{22}(\theta_f, \theta_1) \end{bmatrix},$$
$$\Phi^{\#}(\theta_f, \theta_1) = \Phi^{-T}(\theta_f, \theta_1) = \begin{bmatrix} \Phi^{\#}_{11}(\theta_f, \theta_1) & \Phi^{\#}_{12}(\theta_f, \theta_1) \\ \Phi^{\#}_{21}(\theta_f, \theta_1) & \Phi^{\#}_{22}(\theta_f, \theta_1) \end{bmatrix}. \tag{15}$$

If $\text{cond}(\Phi_{12}(\theta_f, \theta_1)) < \epsilon_{\text{cond}}$ **Then**

$$\begin{aligned} \Delta V(\theta_1) &= \Phi_{12}^{-1}(\theta_f, \theta_1)\big[r_f - \Phi_{11}(\theta_f, \theta_1) r_1 - \Phi_{12}(\theta_f, \theta_1) v_1\big], \\ \Delta V(\theta_f) &= v_f + \big[\Phi_{22}(\theta_f, \theta_1)\Phi_{12}^{-1}(\theta_f, \theta_1)\Phi_{11}(\theta_f, \theta_1) - \Phi_{21}(\theta_f, \theta_1)\big] r_1 \\ &\quad - \Phi_{22}(\theta_f, \theta_1)\Phi_{12}^{-1}(\theta_f, \theta_1) r_f. \end{aligned} \tag{16}$$

Else

Solve polynomial system w.r.t. $(\lambda, \{\Delta v_i\}_{i=1,\dots,f})$

$$\begin{gathered} \lambda^T R(\theta_i) R(\theta_i)^T \lambda = 1, \quad \forall \theta_i \in T_{\text{imp}}, \\ \sum_{\theta_i \in T_{\text{imp}}} \big[R(\theta_i) R^T(\theta_i)\big] \lambda \Delta v_i = u_f, \quad \forall \theta_i \in T_{\text{imp}}, \quad i = 1, \dots, f, \\ \Delta v_i \geq 0, \quad i = 1, \dots, f. \end{gathered} \tag{17}$$

Choose the minimum-fuel solution:

$$\lambda_{\text{init}} = \arg\Big[\min_{\lambda} u_f^T \lambda\Big]. \tag{18}$$

Compute impulses:

$$\begin{aligned} \beta(\theta_i) &= R(\theta_i)^T \lambda_{\text{init}}, \quad \forall \theta_i \in T_{\text{imp}}, \quad i = 1, \dots, f, \\ \Delta V(\theta_i) &= \Delta v_i \beta(\theta_i), \quad \forall \theta_i \in T_{\text{imp}}, \quad i = 1, \dots, f. \end{aligned} \tag{19}$$

(b) **Propagate** primer vector $\lambda_v(\theta)$ on a grid $\Pi = \{\theta_1, \dots, \theta_f\}$:

If $\mathrm{cond}(\Phi^{\#}_{21}(\theta_f, \theta_1)) < \epsilon_{\mathrm{cond}}$ **Then**

$$\lambda_v(\theta_1) = \frac{\Delta V(\theta_1)}{\Delta v_1}, \qquad \lambda_v(\theta_f) = \frac{\Delta V(\theta_f)}{\Delta v_f},$$
$$\lambda_v(\theta) = \Phi^{\#}_{21}(\theta, \theta_1)\Phi^{\#-1}_{21}(\theta_f, \theta_1)\big[\lambda_v(\theta_f) - \Phi^{\#}_{22}(\theta_f, \theta_1)\lambda_v(\theta_1)\big] + \Phi^{\#}_{22}(\theta, \theta_1)\lambda_v(\theta_1). \tag{20}$$

Else

Compute $R(\theta)$ on grid Π and **Propagate** $\lambda_v(\theta)$ via

$$\lambda_v(\theta) = R^T(\theta)\lambda. \tag{21}$$

(c) **Compute**

$$l_{vm} = \max_{\theta \in [\theta_0, \theta_f]} \|\lambda_v(\theta)\| \quad \text{and} \quad \theta_m = \arg\Big[\max_{\theta \in [\theta_0, \theta_f]} \|\lambda_v(\theta)\|\Big].$$

(d) **If** $l_{vm} - 1 < \epsilon_\lambda$ **Then** stop. **The two-impulse trajectory is optimal.**
Else start iterative procedure.

$\epsilon_{1\lambda}$ and $\epsilon_{2\lambda}$ are two different precision values used in the iterative procedure to test the maximum value of the norm of the primer vector with respect to 1. ϵ_{cost} is a parameter used to check the evolution of the cost during the iterative process.

Iterative procedure:
While $(l_{vm} - 1 \geq \epsilon_{1\lambda})$ and $(\mathrm{diff}_{\mathrm{cost}} = |u_f^T \lambda_{\mathrm{iter}} - u_f^T \lambda_{\mathrm{iter}-1}| > \epsilon_{cost}$ or $l_{vm} - 1 \geq \epsilon_{2\lambda})$

(a) iter $\leftarrow$ iter + 1; **Choose** $\theta_a, \theta_b \in T_{\mathrm{imp}}$ such that

$$(\theta_a < \theta_m < \theta_b) \quad \text{and} \quad (\theta_a = \theta_i, \theta_b = \theta_{i+1}).$$

(b) **Modify** $T_{\mathrm{imp}} = T_{\mathrm{imp}} \cup \{\theta_m\}$.

If $\dim(T_{\mathrm{imp}}) > N_{\max}$ **Then Modify** T_{imp} as

(1) **If** $\frac{d\lambda_v(\theta_a)}{d\theta}^T \lambda_v(\theta_a) > 0$ and $\frac{d\lambda_v(\theta_b)}{d\theta}^T \lambda_v(\theta_b) < 0$ **Then**

(i) **If** $\theta_a = \theta_1$ **Then**

$$\theta_b = \theta_m \quad \text{and} \quad T_{\mathrm{imp}} = T_{\mathrm{imp}} - \{\theta_b\}. \tag{22}$$

(ii) **Else**

If $\theta_b = \theta_f$ **Then**

$$\theta_a = \theta_m \quad \text{and} \quad T_{\mathrm{imp}} = T_{\mathrm{imp}} - \{\theta_a\}. \tag{23}$$

(iii) **Else**

$$\theta_a = \theta_b = \theta_m \quad \text{and} \quad T_{\mathrm{imp}} = T_{\mathrm{imp}} - \{\theta_a, \theta_b\} \quad \text{if } \theta_m = (\theta_a + \theta_b)/2, \tag{24}$$

$$\theta_a \quad \text{or} \quad \theta_b = \theta_m \quad \text{and} \quad T_{\text{imp}} = T_{\text{imp}} - \{\theta_a \text{ or } \theta_b\}$$
$$\text{if } |\theta_m - \theta_a| < |\theta_m - \theta_b| \quad \text{or} \quad |\theta_m - \theta_b| < |\theta_m - \theta_a|. \tag{25}$$

(2) **If** $\frac{d\lambda_v(\theta_a)}{d\theta}^T \lambda_v(\theta_a) < 0$ **or** $\frac{d\lambda_v(\theta_b)}{d\theta}^T \lambda_v(\theta_b) > 0$

(i) **If** $\frac{d\lambda_v(\theta_a)}{d\theta}^T \lambda_v(\theta_a) > 0$ **Then**

$$\theta_a = \theta_m \quad \text{and} \quad T_{\text{imp}} = T_{\text{imp}} - \{\theta_a\}. \tag{26}$$

(ii) **If** $\frac{d\lambda_v(\theta_b)}{d\theta}^T \lambda_v(\theta_b) < 0$ **Then**

$$\theta_b = \theta_m \quad \text{and} \quad T_{\text{imp}} = T_{\text{imp}} - \{\theta_b\}. \tag{27}$$

(iii) **If** $\frac{d\lambda_v(\theta_b)}{d\theta}^T \lambda_v(\theta_b) > 0$ **and** $\frac{d\lambda_v(\theta_a)}{d\theta}^T \lambda_v(\theta_a) < 0$

$$\theta_a = \theta_b = \theta_m \quad \text{and} \quad T_{\text{imp}} = T_{\text{imp}} - \{\theta_a, \theta_b\}. \tag{28}$$

(c) **Solve** polynomial system w.r.t. $(\lambda, \{\Delta v_i\}_{i=1,f})$

$$\begin{aligned} &\lambda^T R(\theta_i) R(\theta_i)^T \lambda = 1, \quad \forall \theta_i \in T_{\text{imp}}, \\ &\sum_{\theta_i \in T_{\text{imp}}} \big[R(\theta_i) R^T(\theta_i)\big] \lambda \Delta v_i = u_f, \quad \forall \theta_i \in T_{\text{imp}}, \quad i = 1, \ldots, N, \\ &\Delta v_i \ge 0, \quad i = 1, \ldots, N. \end{aligned} \tag{29}$$

(d) **Choose** the minimum-fuel solution:

$$\lambda_{\text{iter}} = \arg\Big[\min_{\lambda} u_f^T \lambda\Big]. \tag{30}$$

(e) **Compute** impulses:

$$\begin{aligned} \beta(\theta_i) &= R(\theta_i)^T \lambda_{\text{iter}}, \quad \forall \theta_i \in T_{\text{imp}}, \quad i = 1, \ldots, N, \\ \Delta V(\theta_i) &= \Delta v_i \beta(\theta_i), \quad \forall \theta_i \in T_{\text{imp}}, \quad i = 1, \ldots, N. \end{aligned} \tag{31}$$

(f) **Compute** cost difference

$$\text{diff}_{\text{cost}} = \big|u_f^T \lambda_{\text{iter}} - u_f^T \lambda_{\text{iter}-1}\big|. \tag{32}$$

(g) **Compute** $R(\theta)$ on grid Π and **Propagate** $\lambda_v(\theta)$ via

$$\lambda_v(\theta) = R^T(\theta) \lambda_{\text{iter}}. \tag{33}$$

(h) **Compute**

$$l_{vm} = \max_{\theta \in [\theta_1, \theta_f]} \|\lambda_v(\theta)\| \quad \text{and} \quad \theta_m = \arg\Big[\max_{\theta \in [\theta_1, \theta_f]} \|\lambda_v(\theta)\|\Big].$$

Repeat Iterative Procedure until $l_{vm} \le 1$.

The initialization stage and step c of the iterative procedure require solving a system of polynomial equations ((17) in the first case if the transition matrix $\Phi(\theta_f, \theta_1)$ is ill-conditioned and (29) in the iterative procedure) with respect to λ and Δv_i. The set of solutions to the two first sets of equations of this polynomial system are composed of 8 couples of solutions $(\lambda, \{\Delta v_i\}_{i=1,\dots,f})$. Among this set of solutions, only those corresponding to a positive magnitude are kept to compute the minimum-fuel solution. Note that regular algebraic tools for finding all real solutions of multivariate polynomial equations based on formal Gröbner basis computation may fail due to highly complex equations. Here, homotopy continuation methods have been used [26]. In particular, the free software package PHCPack developed by Jan Verschelde [27] is used to solve the system of polynomial equations at each iteration at step c of the iterative procedure, and at the initialization step if necessary. The efficiency of this algorithm is now demonstrated on several different examples.

4 Applications and Numerical Examples

In this section, numerical results obtained from the mixed iterative algorithm, applied to an initial academic example, are compared with previous ones published in the literature [8]. Two additional examples based on more realistic cases borrowed from the ATV program [20] and the PRISMA test bed [3] are provided.[1] In all cases, when the mixed iterative algorithm converges to an N_{it} solution, the Polynomial Rendezvous Delta-V (PRDV) algorithm from [16] is used to certify optimality of this solution for this fixed number of impulses. Only coplanar elliptic rendezvous problems based on the Yamanaka–Ankersen transition matrix [19] are considered for numerical illustration of the results proposed, except for the first case study for which eccentricity $e = 0$. In this last case, the Yamanaka–Ankersen transition matrix reduces to the Hill–Clohessy–Wiltshire transition matrix [17]. Under Keplerian assumptions, the bound of Neustadt [23] on the optimal number of impulses is 4 and therefore $N_{\max} = 4$ in the following. Note also that the algorithm has been successfully applied to the highly elliptic rendezvous mission SIMBOL-X in [24]. Finally, all numerical examples are processed using PHCpack 2.3.52 [26, 27] under Matlab 2010b© running on an Intel® Core(TM) i7 X920 2.0 GHz system with 8 GB RAM.

4.1 Case Study 1

The first example is one of the academic cases of Carter, and is recalled in Table 1. As will be seen in the sequel, this simple example is particularly interesting since it exhibits numerical hurdles to find the optimal solution that is quite surprising for such a simple example.

[1] We would like to thank J.C. Berges from DCT/SB/MO at CNES who provided us with the scenarios for these particular examples.

Table 1 Data for Carter's first example [8]

Eccentricity	$e = 0$
θ_0	0 rad
X_0^T	[1 0 0 0]
θ_f	2π rad
X_f^T	[0 0 0 0]

4.1.1 Analysis of Carter's Solution

The solution proposed in [8] is the minimum-fuel two-impulse solution for fixed thrust locations at the beginning and end of the rendezvous duration. It is made of an initial and final thrusts in opposite directions along the x-axis of the LVLH frame. This solution is analytical in the sense that it is the solution of the linear system:

$$R_{\text{hcw}}(0)\Delta V(0) + R_{\text{hcw}}(2\pi)\Delta V(2\pi) = \phi_{\text{hcw}}^{-1}(2\pi)X_f - \phi_{\text{hcw}}^{-1}(0)X_0 = u_f \tag{34}$$

and may readily be computed as:

$$\Delta V(0) = \begin{bmatrix} \frac{1}{6\pi} & 0 \end{bmatrix}^T, \qquad \Delta V(2\pi) = \begin{bmatrix} -\frac{1}{6\pi} & 0 \end{bmatrix}^T. \tag{35}$$

It could be a reasonable conjecture that this is the minimum-fuel solution, in particular when recalling the following result from [21].

Theorem 4.1 [21] *For HCW rendezvous problems, there is no optimal four-impulse conditions for boundary conditions defined as*

$$X_0^T = \begin{bmatrix} x_0 & z_0 & 0 & 0 \end{bmatrix}, \qquad X_f^T = \begin{bmatrix} 0 & 0 & 0 & 0 \end{bmatrix}.$$

It appears that the solution (35) is not optimal, as may be demonstrated by the associated primer vector that does not satisfy all the necessary conditions of optimality. $\lambda_v(\theta)$ is defined by $\lambda_v(\theta) := R^T(\theta)\lambda$, where $\lambda = [\lambda_1 \ \ \lambda_2 \ \ \lambda_3 \ \ \lambda_4]^T$ must be the solution of the following linear system:

$$\begin{bmatrix} 36\pi^2 + 8 & 4 & 12\pi & -6\pi \\ 4 & 2 & 0 & 0 \\ 12\pi & 0 & 8 & -4 \\ -6\pi & 0 & -4 & 2 \end{bmatrix} \begin{bmatrix} \lambda_1 \\ \lambda_2 \\ \lambda_3 \\ \lambda_4 \end{bmatrix} = \begin{bmatrix} -6\pi \\ 0 \\ 0 \\ 0 \end{bmatrix}. \tag{36}$$

Hence, λ may be parametrized as:

$$\lambda = \begin{bmatrix} -\frac{1}{3\pi} & \frac{2}{3\pi} & \lambda_3 & -1 + 2\lambda_3 \end{bmatrix}^T. \tag{37}$$

If λ is a solution verifying the optimality condition (9), then

$$\left\| \lambda_v(\theta)^c \right\| = \left\| R_{\text{hcw}}^T(\theta)\lambda \right\| < 1, \quad \forall \theta \in]0, 2\pi[. \tag{38}$$

The condition (38) is equivalent to the existence of $\lambda_3 \in \mathbb{R}$ such that $\forall\theta \in]0, 2\pi[$:

$$\begin{aligned}\|\lambda_v(\theta)\|^2 &= \|R_{\text{hcw}}^T(\theta)\lambda\|^2 < 1\\ &= \left[4(\cos\theta - 1)^2 + \sin^2\theta\right]\lambda_3^2 - \frac{4}{\pi}(\cos\theta - 1)[\theta - \pi - \sin\theta]\lambda_3\\ &\quad + \frac{(3(\theta-\pi) - 4\sin\theta)^2 + 4(\cos\theta - 1)^2}{9\pi^2} < 1. \end{aligned} \tag{39}$$

For $\theta = \frac{\pi}{20}$, it is easy to show that the second order polynomial of (39) is always strictly greater than 1, $\forall\lambda_3 \in \mathbb{R}$. Carter's solution is, therefore, not optimal.

4.1.2 Analytical Two-impulse Solution

Let us now consider this problem, without setting the two times of thrusting a priori, but by defining (θ_1, θ_2) as decision variables. The two-point boundary value problem reads as:

$$X_f - \Phi(2\pi, 0)X_0 = \Phi(2\pi, \theta_1)B\Delta V(\theta_1) + \Phi(2\pi, \theta_2)B\Delta V(\theta_2), \tag{40}$$

and is equivalent to the system (41) to be solved:

$$\begin{aligned}&\begin{bmatrix} -6\pi + 3\theta_1 - 4\sin\theta_1 & 2 - 2\cos\theta_1 & -6\pi + 3\theta_2 - 4\sin\theta_2 & 2 - 2\cos\theta_2\\ -2 + 2\cos\theta_1 & -\sin\theta_1 & -2 + 2\cos\theta_2 & -\sin\theta_2\\ -3 + 4\cos\theta_1 & -2\sin\theta_1 & -3 + 4\cos\theta_2 & -2\sin\theta_2\\ 2\sin\theta_1 & \cos\theta_1 & 2\sin\theta_2 & \cos\theta_2 \end{bmatrix}\\ &\times \begin{bmatrix}\Delta V_x(\theta_1)\\ \Delta V_z(\theta_1)\\ \Delta V_x(\theta_2)\\ \Delta V_z(\theta_2)\end{bmatrix} = \begin{bmatrix}-1\\0\\0\\0\end{bmatrix},\\ &M(\theta_1, \theta_2)\Delta V = \varpi_f. \end{aligned} \tag{41}$$

The determinant of $M(\theta_1, \theta_2)$ is:

$$\det M(\theta_1, \theta_2) = 16\sin^2\big((\theta_2 - \theta_1)/2\big) - 3(\theta_2 - \theta_1)\sin(\theta_2 - \theta_1) = g(\theta), \tag{42}$$

where $0 \le \theta = \theta_2 - \theta_1 \le 2\pi$. The function $g(\theta)$ is a strictly positive on $]0, 2\pi[$ and vanishes for 0 and 2π as may be easily verified [6]. Cases $\theta = 0$ and $\theta = 2\pi$ may be excluded for obvious reasons. We get the vector of thrusts as functions of (θ_1, θ_2).

$$\begin{bmatrix}\Delta V_x(\theta_1)\\ \Delta V_z(\theta_1)\\ \Delta V_x(\theta_2)\\ \Delta V_z(\theta_2)\end{bmatrix} = M^{-1}(\theta)\varpi_f = \frac{1}{g(\theta)}\begin{bmatrix}-\sin\theta\\ -4\sin^2(\theta/2)\\ \sin\theta\\ -4\sin^2(\theta/2)\end{bmatrix}. \tag{43}$$

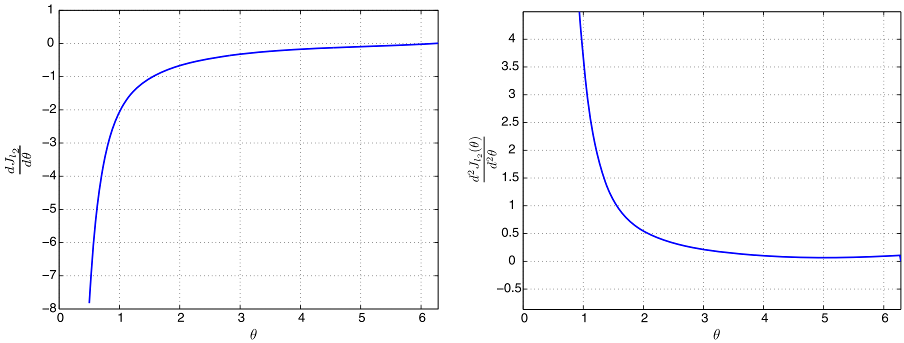

(a) $\frac{dJ_{l_2}(\theta)}{d\theta}$ (b) $\frac{d^2J_{l_2}(\theta)}{d\theta^2}$

Fig. 3 $\frac{dJ_{l_2}(\theta)}{d\theta}$ and $\frac{d^2J_{l_2}(\theta)}{d\theta^2}$ on $(0, 2\pi)$

The minimum-fuel rendezvous problem is equivalent to the parametric optimization problem (44), where θ is the only decision variable.

$$\begin{aligned} &\min_{\theta} \frac{2\sqrt{\sin^2\theta + 16\sin^4(\theta/2)}}{16\sin^2(\theta/2) - 3\theta\sin\theta} = J_{l_2}(\theta) \\ &\text{s.t.} \quad 0 < \theta < 2\pi. \end{aligned} \tag{44}$$

As it is, this problem appears difficult to solve analytically. In fact, (44) is a convex optimization problem for which a minimum may be computed, via the computation of the only zero of its derivative (45) on the interval $(0, 2\pi)$ by a Newton method.

$$\begin{aligned} \frac{dJ_{l_2}(\theta)}{d\theta} = -2\Bigg(&\frac{18\theta + 8\sin(2\theta) - 9\sin(3\theta)/4 - 37\sin\theta/4}{(16\sin^2(\theta/2) - 3\theta\sin\theta)^2\sqrt{16\sin^4(\theta/2) + \sin^2\theta}} \\ &+ \frac{24\theta(2\sin^2(\theta/2) - 1) - 6\theta(2\sin^2(\theta) - 1)}{(16\sin^2(\theta/2) - 3\theta\sin\theta)^2\sqrt{16\sin^4(\theta/2) + \sin^2\theta}}\Bigg). \end{aligned} \tag{45}$$

We get the minimizer θ^* of (44) as

$$\theta^* = 6.230033575529312. \tag{46}$$

The first and second derivatives of $g(\theta)$ are shown in Figs. 3(a) and 3(b), confirming the convexity of the problem on the interval $]0, 2\pi[$.

Finally, the optimal cost and the optimal maneuvers for Carter's example are given by:

$$J_{l_2}(\theta^*) = 0.105954087364712 \begin{bmatrix} \Delta V_x(\theta_1) \\ \Delta V_z(\theta_1) \\ \Delta V_x(\theta_2) \\ \Delta V_z(\theta_2) \end{bmatrix} = \begin{bmatrix} -0.052902333870518 \\ -0.002812512822111 \\ 0.052902333870518 \\ -0.002812512822111 \end{bmatrix}. \tag{47}$$

Table 2 Results of the mixed iterative algorithm for Carter's first example [8]

	Mixed iterative algorithm
θ_i (rad)	$[0\ \ 0.0681\ \ 6.1837\ \ 2\pi]$
$\Delta V(\theta_0)^T$	[0.021453 0.001138]
$\Delta V(\theta_1)^T$	[0.031449 0.001685]
$\Delta V(\theta_2)^T$	[0.006797 0.000364]
$\Delta V(\theta_f)^T$	[0.046105 0.002446]
Fuel cost	0.105954

Fig. 4 Norm of the primer vector and cost evolution

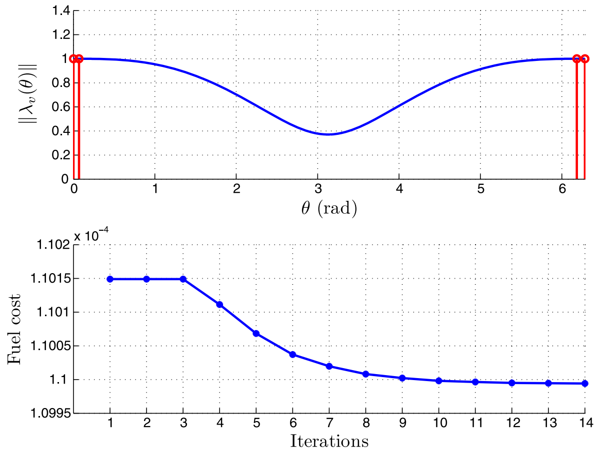

These results show that the optimal two-impulse solution for this example is not unique. There is an infinite number of optimal solutions with the same consumption and a couple of optimal impulse times verifying $(\theta_1^*, \theta_2^*) \in]0, 2\pi - \theta^*[\times]\theta^*, 2\pi[$ with $\theta_2^* - \theta_1^* = \theta^*$.

4.1.3 The Mixed Iterative Algorithm Solution

The results of the mixed iterative algorithm are presented in the Table 2 and clearly show that Carter's solution is indeed not an optimal solution. The mixed algorithm converges after 13 iterations to a four-impulse solution illustrated by Fig. 5(a). The norm of the primer vector and the cost evolution are given in Fig. 4 where $l_{vm} = 1.0000048$.

The distribution of this solution may be defined as two pairs of almost simultaneous impulses at the beginning and at the end of the rendezvous (as is illustrated by the plot of the trajectory in the orbital plane in Fig. 5(b)).

Keeping in mind that the optimal solution has been computed analytically as a two-impulse solution (with one initial and one final coasting period) and recalling the result presented by Theorem 4.1, the result of the mixed iterative algorithm may be analyzed as a tight approximation of the genuine optimal two-impulse solution.

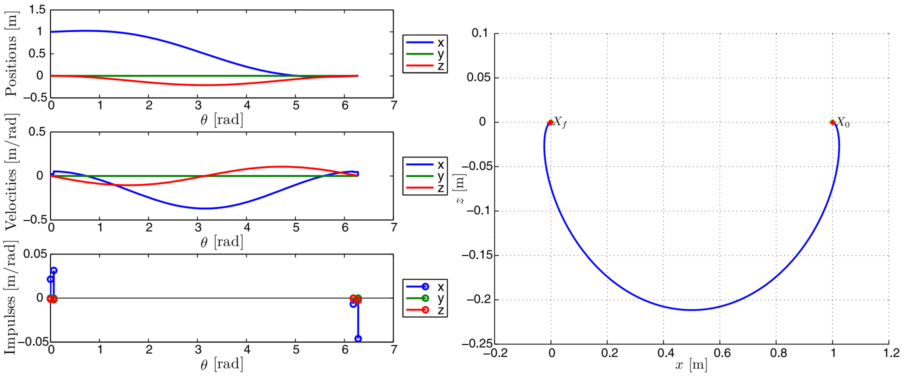

(a) Relatives positions and velocities trajectories and impulses (b) Trajectory of the chaser in the orbital plane (x, z)

Fig. 5 State and control trajectories for the Carter's first case [8]

Table 3 ATV rendezvous characteristics

Semi-major axis	$a = 6763$ km
Inclination	$i = 52$ deg
Argument of perigee	$\omega = 0$ deg
Right ascension of the ascending node	$\Omega = 0$ deg
Eccentricity	$e = 0.0052$
True anomaly	$\theta_0 = 0$ rad
t_0	0 s
$X_0^T = [r_0^T \;\; v_0^T]$	$[-30 \;\; 0.5 \;\; 8.514 \;\; 0]$ km -m/s
t_f	55350 s
$X_f^T = [r_f^T \;\; v_f^T]$	$[-100 \;\; 0 \;\; 0 \;\; 0]$ m -m/s
$N_{\max}$	4

4.2 Case Study 2

Following the first academic numerical example, a more realistic illustration based on the first Automated Transfer Vehicle (ATV) mission [20] is now presented. The ATV is the European unmanned Vehicle capable of performing in-orbit replenishment missions to the International Space Station (ISS). The orbital elements of the target orbit are given in Table 3. Initial, final rendezvous conditions and duration listed in Table 3 are variations of the original scenario that have been provided by CNES. Note that the rendezvous should last for 10 orbit periods.

The mixed iterative algorithm converges to the three-impulse optimal solution within 5 iterations as shown in Table 4. The PRDV algorithm has been applied to this case to certify global optimality of this solution. In addition, the classical two-impulse solution without initial or final coast arc cannot be computed for this example due to the ill-conditioning of the data.

The in-plane trajectory and impulse positions are depicted in Fig. 6(a), while Fig. 6(b) gives the amplitude and locus of the primer vector.

Table 4 Results of the mixed iterative algorithm and two-impulse solution for the ATV case study

	Two-impulse solution	Mixed iterative algorithm
θ_{int} (rad)	–	59.8867
$\Delta V(\theta_0)^T$	–	[−7.55418 0.2336]
$\Delta V(\theta_1)^T$	–	[0.14408 0.00103]
$\Delta V(\theta_f)^T$	–	[0.04166 0.00128]
Fuel cost m/s	–	7.74356

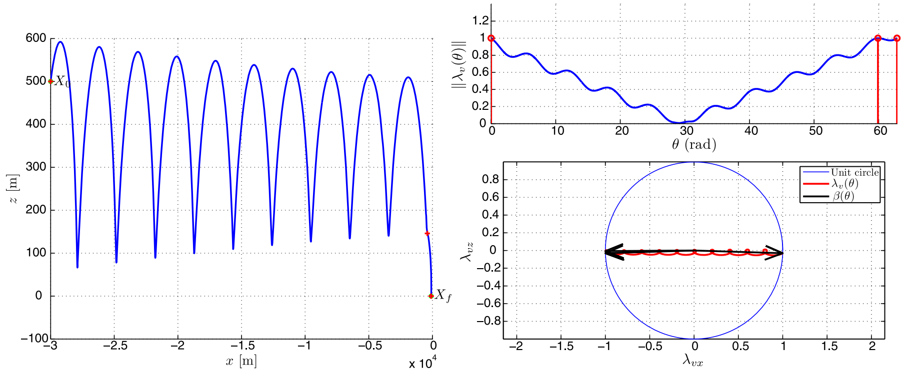

(a) In-plane trajectory and impulse positions * for ATV mission

(b) Primer vector magnitude and locus during ATV mission

Fig. 6 Trajectory and primer vector norm and locus for the ATV mission

4.3 Case Study 3

Finally, an illustration based on PRISMA [3] is now presented. PRISMA programme is a cooperative effort between the Swedish National Space Board (SNSB), the French Centre National d'Etudes Spatiales (CNES), the German Deutsche Zentrum für Luft- und Raumfahrt (DLR) and the Danish Danmarks Tekniske Universitet (DTU) [2]. Launched on June 15, 2010 in Yasny (Russia), it was intended to test in-orbit new guidance schemes (particularly autonomous orbit control) for formation flying and rendezvous technologies. This mission includes the FFIORD experiment led by CNES, which features a rendezvous maneuver (formation acquisition). The orbital elements of the target orbit, as well as initial and final rendezvous conditions, are listed in Table 5.

To save fuel and allow for in-flight testing throughout the FFIORD experiment, the rendezvous maneuver must last several orbits. Duration of the rendezvous is approximately 12 orbital periods for an expected average cost of 20 cm/s [3].

The mixed iterative algorithm achieves optimization within 6 iterations. Global optimality of this four-impulse solution has been established by running the PDRV algorithm.

Figure 7(b) shows primer vector magnitude during transfer. Note the low magnitude of the second and third impulses (0.009 m/s), with respect to the initial and final velocity increments (0.039 m/s), but these velocity increments play a significant role in the optimality of the result. In particular, they provide the right chaser

Table 5 PRISMA rendezvous characteristics

Semi-major axis	$a = 7011$ km
Inclination	$i = 98$ deg
Argument of perigee	$\omega = 0$ deg
Right ascension of the ascending node	$\Omega = 190$ deg
Eccentricity	$e = 0.004$
True anomaly	$\theta_0 = 0$ rad
t_0	0 s
$X_0^T = [r_0^T \;\; v_0^T]$	[10 0 0 0] km -km/s
t_f	70107.1282 s
$X_f^T = [r_f^T \;\; v_f^T]$	[100 0 0 0] m -m/s
$N_{\max}$	4

Table 6 Results of the mixed iterative algorithm and two-impulse solution for the PRISMA case study

	Two-impulse solution	Mixed iterative algorithm
θ_{int}^1 (rad)	–	4.5317
θ_{int}^2 (rad)	–	70.8663
$\Delta V(\theta_0)^T$	[0.04669 −0.04276]	[0.03893 −0.00321]
$\Delta V(\theta_1)^T$	–	[0.009232 −0.00002]
$\Delta V(\theta_2)^T$	–	[0.009232 −0.00002]
$\Delta V(\theta_f)^T$	[−0.046695 0]	[0.03893 −0.00321]
Fuel cost m/s	0.11	0.09659

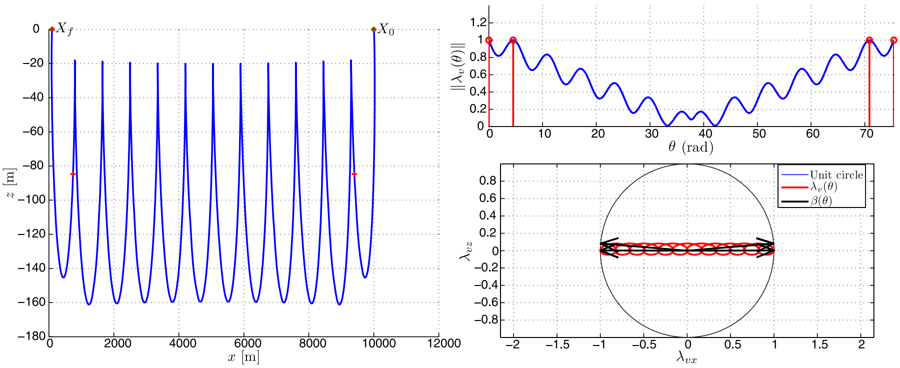

(a) In-plane trajectory and impulse positions * for PRISMA mission (b) Primer vector magnitude and locus during PRISMA mission

Fig. 7 Trajectory and primer vector norm and locus for the PRISMA mission

orientation for the long drift (61665 s) between the second impulse and the third one. The two-impulse strategy, presented in the second column of Table 6, proves to be strongly suboptimal since its fuel cost is 13.83 % greater than the optimal solution (0.09659 m/s). The long drifting period of 61665 s of the optimal solution is clearly illustrated in Fig. 7(a) where the in-plane trajectory and impulse positions are represented. Finally, it is worth noticing that the optimal cost is half the expected average cost of 20 cm/s [3].

5 Conclusion

A new numerical algorithm, based on heuristic rules deduced from the work of [11] and tools from algebraic geometry, has been proposed to address the issue of time-fixed optimal rendezvous in a linear setting. This algorithm is a mixed iterative algorithm optimizing over the number of impulses with a low numerical complexity, mainly consisting in the solution of a small size polynomial system of equations.

A first extension of this work would be to derive a formal proof of the convergence of this heuristic algorithm. This convergence analysis could demonstrate the efficiency of the logic on which is based the algorithm or concur to improve it. In addition, its numerical behavior may probably be improved by considering a tailored tool for the solution of the system of polynomial equations. Despite the good numerical results presented, some improvement can still be expected if more sophisticated transition matrices (including orbital perturbation effects) are used such as atmospheric drag or gravity harmonics term J_2. It will imply to work out generalizations of the work of Lion and Handelsman to new relative dynamics models such the ones given in [28, 29]. Another avenue of research deals with the extension of this algorithm for optimal trajectory planning with collision avoidance constraints by considering path-constraints for impulsive trajectories.

Acknowledgements This work was supported by CNES Grant R-S07/VF-0001-065. The Authors would like to thank Marine Feron for her careful reading of our manuscript and providing us with her comments and suggestions to improve the quality of the writing.

References

1. Hughes, S.P., Mailhe, L.M., Guzman, J.J.: A comparison of trajectory optimization methods for the impulsive minimum fuel rendezvous problem. In: Gravseth, I.J., Culp, R.D. (eds.) Advances in Guidance and Control. Advances in the Astronautical Sciences, vol. 113, pp. 85–104. AIAA, New York (2003)
2. Larsson, R., Berge, S., Bodin, P., Jonsson, U.: Fuel efficient relative orbit control strategies for formation flying and rendezvous within PRISMA. In: Proceedings of the 29th Annual AAS Rocky Mountain Guidance and Control Conference, Breckenridge, Colorado, USA, pp. 25–40 (2006)
3. Berges, J.C., Cayeux, P., Gaudel-Vacaresse, A., Messygnac, B.: CNES approaching guidance experiment within FFIORD. In: Proceedings of the 21st International Symposium on Space Flight Dynamics, Annapolis, Maryland, USA, pp. 24–28 (2007)
4. Delpech, M., Berges, J.C., Djalal, S., Guidotti, P.Y., Christy, J.: Preliminary results of the vision based rendezvous and formation flying experiments performed during the PRISMA extended mission. In: Proceedings of the 1st IAA Conference on Dynamics and Control of Space Systems, DYCoSS'2012, Porto, Portugal (2012)
5. Lawden, D.F.: Optimal Trajectories for Space Navigation. Butterworth, London (1963)
6. Prussing, J.E.: Optimal multiple-impulse orbital rendezvous. Ph.D. Thesis, Massachusetts Institute of Technology, Cambridge, MA (1967)
7. Prussing, J.E.: Illustration of the primer vector in time-fixed orbit transfer. AIAA J. **7**(6), 1167–1168 (1969)
8. Carter, T.E.: Optimal impulsive space trajectories based on linear equations. J. Optim. Theory Appl. **70**(2), 277–297 (1991)

9. Carter, T.E.: Necessary and sufficient conditions for optimal impulsive rendezvous with linear equations of motion. Dyn. Control **10**, 219–227 (2000)
10. Carter, T.E., Brient, J.: Linearized impulsive rendezvous problem. J. Optim. Theory Appl. **86**(3), 553–584 (1995)
11. Lion, P.M., Handelsman, M.: Primer vector on fixed-time impulsive trajectories. AIAA J. **6**(1), 127–132 (1968)
12. Jezewski, D.J., Rozendaal, H.L.: An efficient method for calculating optimal free-space n-impulse trajectories. AIAA J. **6**(11), 2160–2165 (1968)
13. Jezewski, D.J.: Primer vector theory applied to the linear relative-motion equations. Optim. Control Appl. Methods **1**, 387–401 (1980)
14. Prussing, J.E.: Primer vector theory and applications. In: Conway, B.A. (ed.) Spacecraft Trajectory Optimization. Cambridge University Press, Cambridge (2010)
15. Prussing, J.E., Chiu, J.H.: Optimal multiple-impulse time-fixed rendezvous between circular orbits. J. Guid. Control Dyn. **9**(1), 17–22 (1986)
16. Arzelier, D., Kara-Zaitri, M., Louembet, C., Delibasi, A.: Using polynomial optimization to solve the fuel-optimal impulsive rendezvous problem. J. Guid. Control Dyn. **34**(5), 1567–1572 (2011)
17. Clohessy, W.H., Wiltshire, R.S.: Terminal guidance system for satellite rendezvous. J. Aerosp. Sci. **27**(9), 653–658 (1960)
18. Tschauner, J., Hempel, P.: Rendevous zu einem in elliptischer Bahn umlaufenden Ziel. Acta Astronaut. **II**(2), 104–109 (1965)
19. Yamanaka, K., Ankersen, F.: New state transition matrix for relative motion on an arbitrary elliptical orbit. J. Guid. Control Dyn. **25**(1), 60–66 (2002)
20. Labourdette, P., Julien, E., Chemama, F., Carbonne, D.: ATV Jules Verne mission maneuver plan. In: Proceedings of the International Symposium on space flight dynamics, Toulouse, France (2008)
21. Carter, T.E., Alvarez, S.A.: Quadratic-based computation of four-impulse optimal rendezvous near circular orbit. J. Guid. Control Dyn. **23**(1), 109–117 (2000)
22. Prussing, J.E.: Optimal impulsive linear systems: Sufficient conditions and maximum number of impulses. J. Astronaut. Sci. **43**(2), 195–206 (1995)
23. Neustadt, L.W.: A general theory of minimum-fuel space trajectories. SIAM J. Control **3**(2), 317–356 (1965)
24. Kara-Zaitri, M., Arzelier, D., Louembet, C.: Mixed iterative algorithm for solving impulsive time-fixed rendezvous problem. In: Proceedings of the AIAA Guidance, Navigation, and Control Conference, Toronto, Canada (2010)
25. Guzmán, J.J., Mailhe, L.M., Schiff, C., Hughes, S.P., Folta, D.C.: Primer vector optimization: survey of theory, new analysis and applications. In: Proceedings of the 53rd International Astronautical Congress, Houston, Texas, USA, pp. 10–19 (2002)
26. Verschelde, J.: Homotopy methods for solving polynomial systems. In: Proceedings of the International Symposium on Symbolic and Algebraic Computations, Beijing, China (2005)
27. Verschelde, J.: Algorithm 795: PHCpack: a general-purpose solver for polynomial systems by homotopy continuation. ACM Trans. Math. Softw. **25**(2), 251–276 (1999)
28. Gim, D.W., Alfriend, K.T.: State transition matrix of relative motion for the perturbed noncircular reference orbit. J. Guid. Control Dyn. **26**(6), 956–971 (2003)
29. Yamada, K., Kimura, M.: New state transition matrix for formation flying in J_2-perturbed elliptic orbits. J. Guid. Control Dyn. **35**(2), 536–547 (2012)